Neutron-proton asymmetry dependence of nuclear temperature with intermediate mass fragments

X. Liu (刘星泉),[1,2] H. Zheng (郑华),[3] R. Wada,[4,5] W. Lin (林炜平),[1,*] M. Huang (黄美容),[6] P. Ren (任培培),[1] G. Qu (曲国峰),[1] J. Han (韩纪锋),[1] M. R. D. Rodrigues,[7] S. Kowalski,[8] T. Keutgen,[9] K. Hagel,[4] M. Barbui,[4] A. Bonasera,[4,10] and J. B. Natowitz[4]

[1]*Key Laboratory of Radiation Physics and Technology of the Ministry of Education, Institute of Nuclear Science and Technology, Sichuan University, Chengdu 610064,China*

[2]*Institute of Modern Physics, Chinese Academy of Sciences, Lanzhou 730000, China*

[3]*School of Physics and Information Technology, Shaanxi Normal University, Xi'an 710119, China*

[4]*Cyclotron Institute, Texas A&M University, College Station, Texas 77843, USA*

[5]*School of Physics, Henan Normal University, Xinxiang 453007, China*

[6]*College of Physics and Electronics information, Inner Mongolia University for Nationalities, Tongliao, 028000, China*

[7]*Instituto de Física, Universidade de São Paulo, Caixa Postal 66318, CEP 05389-970, São Paulo, SP, Brazil*

[8]*Institute of Physics, Silesia University, Katowice, Poland*

[9]*FNRS and IPN, Université Catholique de Louvain, B-1348 Louvain-Neuve, Belgium*

[10]*Laboratori Nazionali del Sud, INFN, via Santa Sofia, 62, 95123 Catania, Italy*

(Received 27 April 2019; revised manuscript received 27 August 2019; published 4 December 2019)

The dependence of the nuclear temperature on the source neutron-proton (N/Z) asymmetry is experimentally investigated with the intermediate mass fragments (IMFs) generated from thirteen reaction systems with different N/Z asymmetries, ^{64}Zn on ^{112}Sn and ^{70}Zn, ^{64}Ni on ^{112,124}Sn, ^{58,64}Ni, ^{197}Au, ^{232}Th at 40 MeV/nucleon. The apparent source temperatures for these systems are determined from the measured IMF yields from the intermediate velocity sources using eight carbon-related double isotope ratio thermometers. A rather weak N/Z asymmetry dependence of the source temperature is qualitatively inferred from the extracted N/Z asymmetry dependence of the apparent temperature and that of the relative temperature change by the sequential decay effects with the help of the theoretical simulations. The present result is compared with those from other available experiments.

DOI: 10.1103/PhysRevC.100.064601

I. INTRODUCTION

The neutron-proton (N/Z) asymmetry dependence of the nuclear caloric curve, namely, the dependence of the temperature relative to the excitation energy on the N/Z asymmetry of the reaction system (or the fragmenting source), provides crucial information on the N/Z asymmetry dependence of the nuclear forces, the properties of excited nuclei and the postulated nuclear liquid-gas phase transition [1–4]. However, large uncertainties in the N/Z asymmetry dependence of the nuclear caloric curve still remain, due to the relatively scarce experimental data and the conflicting conclusions drawn from the experiments and theoretical studies. For the experimental studies on the N/Z asymmetry dependence of the nuclear temperature, Sfienti *et al.* [5], Trautmann *et al.* [6], and Wuenschel *et al.* [7] found that the experimentally extracted source temperatures show a rather weak dependence on the N/Z asymmetry of the fragmenting source. In contrast, McIntosh *et al.* [8] found that the extracted temperatures are notably higher for relatively proton-richer systems than those for neutron-richer systems. In theoretical works, some predicted that limiting temperatures, defined as the plateau temperature of the caloric curve, are higher for neutron-poor systems [9], whereas others made the opposite prediction [10–12]. These experimental and theoretical ambiguities are attributed to various causes, such as the application of different thermometers which may reflect different fragmentation mechanisms [8,13–17], different modeling assumptions in theoretical calculations, among others [9]. To address these issues and pursue a consistent description for the N/Z asymmetry dependence of the nuclear temperature, further effort is still required in both experimental and theoretical studies.

Light charged particles (LCPs) have been the primary temperature probe in the previous studies [18]. As intermediate mass fragments (IMFs) are copiously produced through the multifragmentation process in intermediate-energy heavy-ion collisions [19], they provide an additional opportunity to study the temperature behavior as well. We recently experimentally extracted the temperature of the fragmenting source from the IMF isotope distributions with a self-consistent method [20–24] and then studied the incident energy dependence of the temperature [25]. These works provide us an opportunity to pursue the source N/Z asymmetry dependence of the nuclear temperature using IMFs as a probe.

In this work, we use IMFs from thirteen reaction systems with different N/Z asymmetries to investigate the N/Z asymmetry dependence of the nuclear temperature. The

*linwp1204@scu.edu.cn

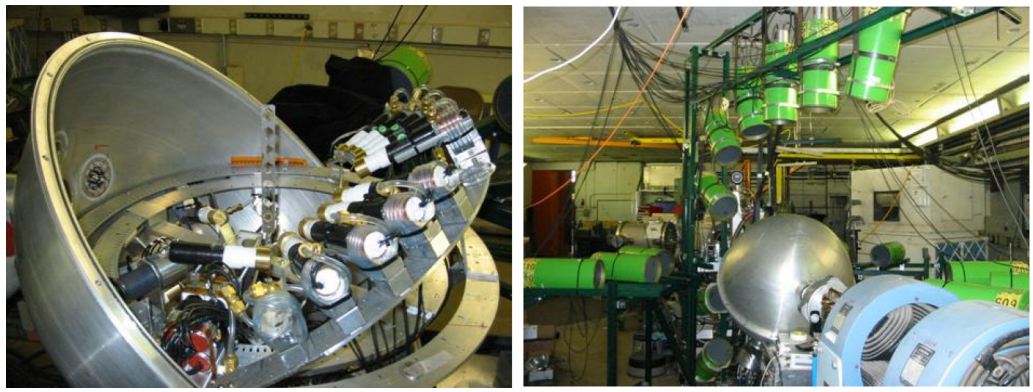

FIG. 1. Physical views of the detector setup. Left: the IMF telescope and 16 CsI detectors were arranged around the target inside the spherical scattering chamber; Right: the 16 DEMON detectors for neutron measurement were arranged outside the chamber. The pictures were taken before the runs and the detector arrangements in the left figure are slightly different from the actual runs. Two figures have not been digitally altered.

double isotope ratio thermometer [26] is adopted to extract the temperatures from the IMF isotope yields. As the measured isotope yields are perturbed by the sequential decay, it may result in a serious inaccuracy in the temperature determination using the double isotope ratio thermometer, even though the sequential decay effect has been considered in some extent [5,27,28]. Therefore, the experimentally inferred temperature from the double isotope ratio thermometer is called "apparent temperature," whereas that before the sequential decays is called "real (source) temperature." However, the double isotope ratio thermometer has been widely used to study thermodynamic properties of fragmenting sources, i.e., temperature as a function of excitation energy (caloric curve) [18,27,29,30], N/Z asymmetry dependence [5,6,17,31], and time evolution during the collisions [32]. These studies indicate that even though the temperature values (with or without sequential corrections) from different double isotope ratio thermometers are not always consistent, the double isotope ratio thermometer used as a relative thermometer could reflect the general behaviors of the nuclear temperature dependence on excitation energy, source N/Z asymmetry, time evolution and among others qualitatively. Following the strategy of these previous works, the N/Z asymmetry dependence of the real source temperature is therefore studied using the double isotope ratio thermometer in this work. Theoretical model calculations are also performed to compare to the experimental results and provide insight into the sequential decay effect. This article is organized as follows. In Sec. II, we briefly describe the experiment and data analysis. In Sec. III, a description for the double isotope ratio formalism is given. In Sec. IV, the N/Z asymmetry dependence of the apparent temperature is determined. In Secs. V and VI, discussion and summary are given.

II. EXPERIMENT AND DATA ANALYSIS

A. Experiment

The experiment was performed at the K-500 superconducting cyclotron facility at Texas A&M University. ^{64,70}Zn and ^{64}Ni beams were used to irradiate ^{58,64}Ni, ^{112,124}Sn, ^{197}Au, and ^{232}Th targets at 40 MeV/nucleon. Thirteen reaction systems, ^{64}Zn on ^{112}Sn and ^{70}Zn, ^{64}Ni on ^{112,124}Sn, ^{58,64}Ni, ^{197}Au, ^{232}Th, were analyzed in this work. The physical views of the detector setup used in the experiment are presented in Fig. 1. IMFs were detected by a detector telescope placed at 20° in the spherical scattering chamber (left of Fig. 1). The telescope consisted of four Si detectors. Each Si detector was 5 × 5 cm. The nominal thicknesses were 129, 300, 1000, 1000 μm, respectively. All four Si detectors were segmented into four sections and each quadrant had a 5° opening in the polar angle. During the experiment, the telescope signals were taken inclusively as the main trigger for all detected events. Typically $6 \sim 8$ isotopes for atomic numbers as high as $Z = 18$ were clearly identified with energy thresholds of $4 \sim 10$ MeV/nucleon, using the $\Delta E - E$ technique for any two consecutive detectors. Mass identification of the isotopes was made using a range-energy table [33]. Besides IMFs, the LCPs in coincidence with IMFs were also measured using 16 single-crystal CsI(Tl) detectors of 3 cm length set around the target at angles between $\theta_{\rm Lab} = 27°$ and $\theta_{\rm Lab} = 155°$. Sixteen detectors of the Belgian-French neutron detector array DEMON (Detecteur Modulaire de Neutrons, right of Fig. 1) [34] outside the chamber were used to measure neutrons, covering polar angles of $15° \leqslant \theta_{\rm IMF-n} \leqslant 160°$ between the telescope and the neutron detectors. Data analysis with these LCP and neutrons were presented in Refs. [21,35]. In this article, we focus on the data analysis of the measured IMFs.

B. Event identification

Since the IMFs were taken inclusively, the angle of the IMF telescope was set carefully to optimize the IMF yields. The consideration was that the angle should be small enough to ensure that sufficient IMF yields are obtained above the detector energy threshold, as well as large enough to minimize contributions from peripheral collisions. For this purpose, simulations of the antisymmetrized molecular dynamics model (AMD) [36] incorporating the statistical decay code GEMINI as an afterburner [37] (used in the previous work [38]) were performed. Figure 2 presents the calculated impact

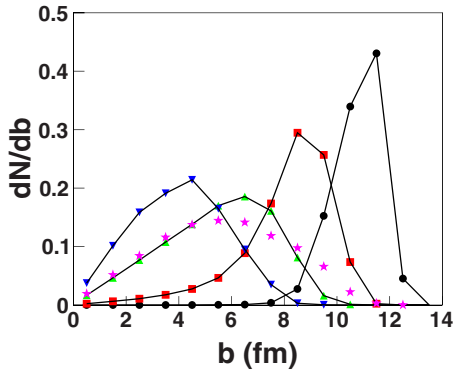

FIG. 2. Simulated impact parameter distributions for violent (downward triangles), semi-violent (upward triangles), semi-peripheral (squares) and peripheral (dots) collisions of ^{64}Zn + ^{112}Sn at 40 MeV/nucleon. Stars indicate the events in which at least one IMF ($Z \geqslant 3$) is emitted at 15°–25°. The summed distribution for a given event class is normalized to 1. The figure is taken from Ref. [39] with permission.

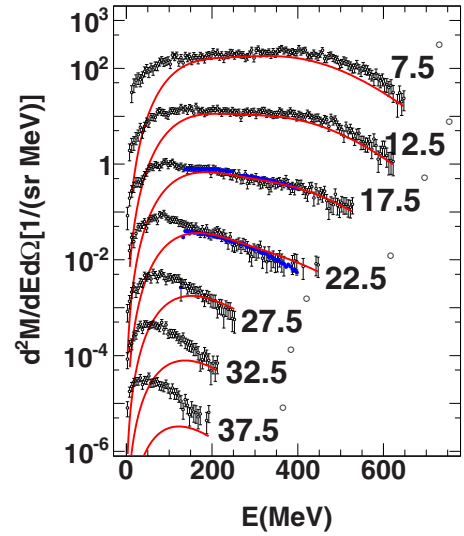

FIG. 3. Experimental ^{16}O energy spectra for the system of ^{64}Zn + ^{112}Sn at 40 MeV/nucleon (closed circles) are compared with those of AMD+GEMINI simulation (open circles). The spectra of the AMD+GEMINI simulation were obtained from the semi-violent collisions. The curves are the results of the moving source fit, for which the parameters were determined from the experimental spectra at 17.5° and 22.5°. Angles are given in the figure and the absolute Y scale is corresponding to the bottom spectra and the spectra are multiplied by a factor of 10 from the bottom to the top. The figure is taken from Ref. [39] with permission.

parameter distributions for the system of ^{64}Zn + ^{112}Sn at 40 MeV/nucleon. In this figure, the violence of the reaction for each event was determined in the same way as that in Ref. [38], in which the multiplicity of light particles, including neutrons, and the transverse energy of light charged particles were used. The resultant impact parameter distributions for each class of events are shown together with that of the events in which at least one IMF is emitted at the polar angles within 15°–25°. As seen in the figure, the distribution of the events selected by this IMF trigger is similar to that of semiviolent collisions.

C. Source characterization and multiplicity determination

To further characterize the fragmenting source to isolate the reaction mechanisms involved in the reaction products, a moving source fit [40] was employed. In the moving source fit, the sources were classified as projectile-like (PLF), intermediate-velocity (IV) (also called as nucleon-nucleon-like (NN) [41]), and target-like (TLF) sources according to the source velocity. The isotope spectra of IMFs from 15° to 25° were fitted using a single IV source. Using a source with a smeared source velocity around half the beam velocity, the fitting parameters were first determined from the spectrum summed over all isotopes for a given Z under an assumption of $A = 2Z$. Then all extracted parameters except the normalizing yield parameter were applied to the other individual isotopes with the same Z, and the multiplicity for each given isotope was obtained as a parameter from the moving source fits. In Fig. 3, the experimental energy spectra of ^{16}O at 17.5° and 22.5° are presented by closed circles as an example and compared with those from the semiviolent collisions predicted by AMD+GEMINI simulations. The experimental spectra at 17.5° and 22.5° are reproduced reasonably by the AMD+GEMINI simulation. The experimental spectra at 17.5° and 22.5° were fitted using a single IV source with the aid over the MINUIT program in the Cern ROOT library. Solid red curves correspond to the fit results. Good agreement between the experimental results (as well as those from the AMD+GEMINI simulation) and the fits at 17.5° and 22.5° is obtained, although significant deviation appears on the lower energy part of the spectrum. This deviation is attributed to the TLF component. The TLF component could not be fully measured in this experiment due to the high energy thresholds for IMFs. We also note that a small enhancement in the AMD+GEMINI spectra above the moving source fit at forward angles which is attributed to the PLF component. In Fig. 4, the Oxygen isotope multiplicities of the IV source component determined from the single-source moving source fits are presented with the error bars which are described below. The corresponding results from the three-source moving source fits for the AMD+GEMINI spectra are also plotted for comparison. The close agreement between both results suggests a good assumption of single-source fit to the present experimental IMF spectra.

The errors of the isotope yields from the moving source fits were evaluated by performing different optimizations with different initial values within a wide range, including source velocity, energy slope and among others, rather than the errors given by the MINUIT from the fits, because there were many local minima for the multiple parameter fits. Rather large errors (around ±10%) were assigned for the multiplicity of the IV source for IMFs, originating from the source fit. Similar moving source fits were also applied to the energy spectra of LCPs and neutrons. The extracted IV-source multiplicities of neutrons, LCPs and IMFs for all thirteen reactions are given in the Supplemental Material of this article [42]. Only the

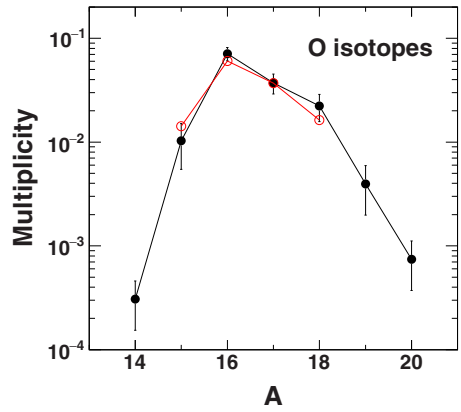

FIG. 4. Oxygen isotope multiplicity distribution determined from the moving source fits for the spectra of ^{64}Zn + ^{112}Sn at 40 MeV/nucleon at 17.5° and 22.5° (closed circles), together with those from the three-source moving source fits for the corresponding AMD+GEMINI spectra (open circles). See details about the experimental error evaluation in the text. Also note that no error is presented for the AMD+GEMINI case.

multiplicities of the fragments emitting from the IV source were used in the following investigation of the source N/Z asymmetry dependence of the nuclear temperature.

III. DOUBLE ISOTOPE RATIO THERMOMETER FORMALISM

The double isotope ratio thermometer was first proposed by Albergo *et al.* [26]. Under the assumption that thermal equilibrium may be established between free nucleons and composite fragments contained within a certain freezeout volume V and a temperature T, the density of an isotope with A nucleons and Z protons (A, Z) may be expressed as

$$\rho(A,Z) = \frac{N(A,Z)}{V} = \frac{A^{3/2}\omega(A,Z)}{\lambda_T^3}\exp\left[\frac{\mu(A,Z)}{T}\right], \quad (1)$$

where $N(A, Z)$ is the number of isotope (A, Z) within the volume V; $\lambda_T = h/(2\pi m_0 T)^{1/2}$ is the thermal nucleon wavelength, where m_0 is the nucleon mass; $\omega(A, Z)$ is the internal partition function of the isotope (A, Z) and related to the ground- and excited-state spins (practically, $\omega(A, Z)$ is limited to that at the ground state [26]); $\mu(A, Z)$ is the chemical potential of the isotope (A, Z). In chemical equilibrium, $\mu(A, Z)$ is expressed as

$$\mu(A,Z) = Z\mu_p + (A-Z)\mu_n + B(A,Z), \quad (2)$$

where $B(A, Z)$ is the binding energy of the isotope (A, Z). μ_p and μ_n are the chemical potentials of free protons and free neutrons, respectively. Calculating the densities of free protons and neutrons, ρ_p and ρ_n, in the same volume using Eqs. (1) and (2), performing transforms to obtain μ_p and μ_n, and then inserting μ_p and μ_n back into Eq. (1), one obtains

$$\begin{aligned}\rho(A,Z) &= \frac{N(A,Z)}{V} \\ &= \frac{A^{3/2}\omega(A,Z)\lambda_T^{3(A-1)}}{(2s_p+1)^Z(2s_n+1)^{A-Z}}\rho_p^Z\rho_n^{A-Z}\exp\left[\frac{B(A,Z)}{T}\right], \end{aligned} \quad (3)$$

where s_p and s_n are the spins of the free proton and neutron, respectively. The ratio between the measured yields of two different isotopes is then

$$\begin{aligned}\frac{Y(A,Z)}{Y(A',Z')} &= \frac{\rho(A,Z)}{\rho(A',Z')} \\ &= \left(\frac{A}{A'}\right)^{3/2}\left(\frac{\lambda_T^3}{2}\right)^{A-A'}\frac{\omega(A,Z)}{\omega(A',Z')}\rho_p^{(Z-Z')}\rho_n^{(A-Z)-(A'-Z')} \\ &\quad\times\exp\left[\frac{B(A,Z)-B(A',Z')}{T}\right]. \end{aligned} \quad (4)$$

The free proton density can be calculated from the yield ratio of two fragments with only one proton difference, such as (A, Z) and $(A + 1, Z + 1)$,

$$\begin{aligned}\rho_p &= C\left(\frac{A}{A+1}T\right)^{3/2}\frac{\omega(A,Z)}{\omega(A+1,Z+1)} \\ &\quad\times\exp\left[\frac{B(A,Z)-B(A+1,Z+1)}{T}\right]\frac{Y(A+1,Z+1)}{Y(A,Z)}, \end{aligned} \quad (5)$$

where C is the constant related to the unit conversion. Analogously, the free neutron density is calculated from the yield ratio of two fragments with only one neutron difference, such as (A, Z) and $(A + 1, Z)$,

$$\begin{aligned}\rho_n &= C\left(\frac{A}{A+1}T\right)^{3/2}\frac{\omega(A,Z)}{\omega(A+1,Z)} \\ &\quad\times\exp\left[\frac{B(A,Z)-B(A+1,Z)}{T}\right]\frac{Y(A+1,Z)}{Y(A,Z)}. \end{aligned} \quad (6)$$

For a given temperature T, the same free proton (or neutron) density must be evaluated from Eq. (5) [or Eq. (6)]. Choosing two ratios with one proton (or neutron) excess, one can deduce the relation between T and the experimental yield ratios as

$$T = \frac{B_{\rm diff}}{\ln(aR)}, \quad (7)$$

and the error of T, δT, is deduced as

$$\delta T = \frac{B_{\rm diff}}{\ln^2(aR)}\frac{\delta R}{R}, \quad (8)$$

where $R = (Y_1/Y_2)/(Y_3/Y_4)$ is the double isotope yield ratio of the ground states for isotope pairs (1,2) and (3,4), and δR is the error of R. One can find from Eq. (8) that δT depends on both $B_{\rm diff}/\ln^2(aR)$ and $\delta R/R$. In this work, the experimental (1,2) and (3,4) ratios with same one-neutron excess are adopted. $B_{\rm diff}$ is the binding energy difference, $B_{\rm diff} = (B_1 - B_2) - (B_3 - B_4)$. a is the statistical weighting factor and is defined as

$$a = \frac{\omega_3/\omega_4}{\omega_1/\omega_2}\left[\frac{A_3/A_4}{A_1/A_2}\right]^{1.5}, \quad (9)$$

where $\omega_i = 2S_i + 1$ and S_i is the ground-state spin of the ith isotope and A_i is the mass number of the ith isotope. In the actual temperature determination, isotope pairs with large $B_{\rm diff}$ values are recommended [43]. Following Ref. [43], the IMF temperatures in this work are therefore determined using eight

TABLE I. List of the parameters for the eight carbon-related thermometers used in the present work.

ID	Isotope ratio	$B_{\rm diff}$ (MeV)	a
1	^{6,7}Li/^{11,12}C	11.47	5.90
2	^{7,8}Li/^{11,12}C	16.69	5.36
3	^{9,10}Be/^{11,12}C	11.91	1.03
4	^{11,12}B/^{11,12}C	15.35	3.00
5	^{12,13}B/^{11,12}C	13.84	5.28
6	^{12,13}C/^{11,12}C	13.77	7.92
7	^{13,14}C/^{11,12}C	10.54	1.96
8	^{15,16}N/^{11,12}C	16.23	9.67

carbon-related isotope ratios with $B_{\rm diff} > 10$ MeV. The ratios used for constructing the thermometers and their associated $B_{\rm diff}$ and a values are listed in Table I.

IV. RESULTS: *N/Z* ASYMMETRY DEPENDENCE OF APPARENT TEMPERATURE

The resultant apparent temperature values from the eight thermometers are plotted in Fig. 5 as a function of the source N/Z asymmetry, $\delta_{\rm IV} = (N_{\rm IV} - Z_{\rm IV})/A_{\rm IV}$, where $N_{\rm IV}$, $Z_{\rm IV}$, and $A_{\rm IV}$ are the neutron, proton, and mass of the fragmenting source calculated from summing over the experimentally measured IV component yields of neutrons, LCPs, and IMFs with Z up to 18. Errors shown in the figure are calculated from the isotope multiplicity errors using Eq. (8). Note again that as the experimental yields which result from the sequential decay are used in Eq. (7), the calculated temperatures in this section are the apparent temperatures. The extracted apparent temperatures from all eight thermometers shown in the figure exhibit almost no dependence on $\delta_{\rm IV}$. A global fit to the eight $T_{\rm app}$ versus $\delta_{\rm IV}$ plots with linear functions with one common slope $k_{\rm app}$ and individual intercepts is performed. $k_{\rm app}$ in the fit reflects the average trend of the apparent temperature as $\delta_{\rm IV}$ increases, whereas the individual intercepts are sensitive to the extracted values of apparent temperature. A common slope, $k_{\rm app} = -0.5 \pm 0.1$ MeV, is obtained, where the error is the fitting error. The small $k_{\rm app}$ value indicates that the apparent temperature decreases weakly as the source N/Z asymmetry increases, that is, the apparent temperature decreases ∼0.07 MeV on average as $\delta_{\rm IV}$ increases from 0.14 to 0.27 for the present source N/Z asymmetry region. Different intercept values of ∼3–6 MeV is also obtained for the different thermometers in contrast.

V. DISCUSSION

A. Temperature from AMD simulations for ^{64}Zn + ^{112}Sn

Taking the reaction system of ^{64}Zn + ^{112}Sn as an example, the apparent temperature values from the eight thermometers are compared in Fig. 6, together with those from the AMD+GEMINI simulation, $T_{\rm app,AMD}$. The AMD+GEMINI events with an impact parameter range of 0–8 fm are used in this analysis. An approximated isotope selection for characterizing the IV source, $E_{\rm lab}/A > 5$ MeV and $5^\circ < \theta_{\rm lab} < 25^\circ$, is applied to these events. This selection method has been verified in our previous work [21]. Errors of the apparent temperature values from the AMD+GEMINI simulated events, which are within symbols, are evaluated from the statistical

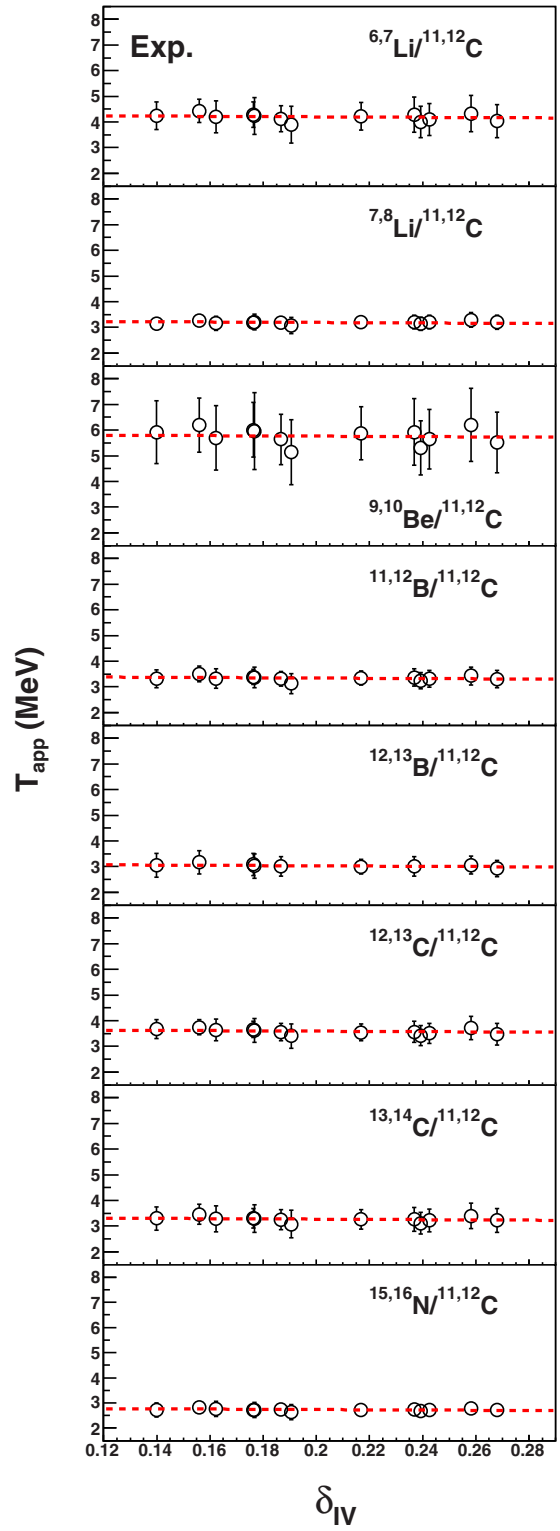

FIG. 5. Apparent temperatures $T_{\rm app}$ from the eight carbon-related double isotope ratio thermometers as a function of source N/Z asymmetry $\delta_{\rm IV}$. Red dashed lines are the global fits with linear functions with one common slope $k_{\rm app}$ and different intercepts.

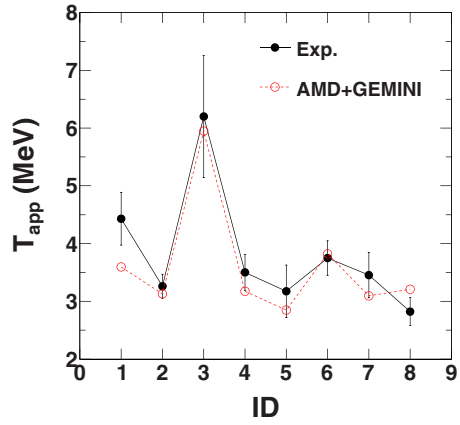

FIG. 6. Apparent temperatures from the eight carbon-related double isotope ratio thermometers from the $^{64}Zn + ^{112}Sn$ system as a function of the thermometer ID given in Table I. Dots and circles are those from the experiment and the AMD+GEMINI simulations, respectively. Lines are guides for the eyes.

errors of the generated events. In the figure, the experimental and theoretical apparent temperatures are rather consistent, though a few simulated values are out of the experimental error bars. Both show a significant apparent temperature fluctuation of ∼3–6 MeV, which corresponds to fluctuations in the heights of the horizontal dashed lines at a given value of δ_{IV} in Fig 5.

In Fig. 7, the extracted real temperature, T_{AMD}, from the primary isotope yields of the AMD simulations for the $^{64}Zn + ^{112}Sn$ system, the above AMD apparent temperature, $T_{app,AMD}$, and the difference between these two temperatures, ΔT ($\Delta T = T_{app,AMD} - T_{AMD}$), are shown for the different thermometers. The same event and isotope selections as those of the AMD+GEMINI are applied to the AMD events [21], though this is only approximately true for the primary fragments. The extracted source temperature for the eight

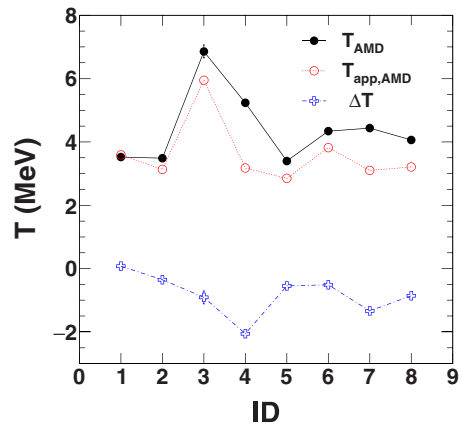

FIG. 7. Temperatures from the eight carbon-related double isotope ratio thermometers from the primary and secondary isotope yields, T_{AMD} and $T_{app,AMD}$, of the $^{64}Zn + ^{112}Sn$ system, together with the relative temperature change, ΔT, between $T_{app,AMD}$ and T_{AMD}, as a function of the thermometer ID given in Table I. Lines are guides for the eyes.

thermometers from the primary yields varies from ∼3.5 MeV to ∼7 MeV shown by solid circles in the figure. This result reveals an incredibility for the double isotope ratio thermometers that it does not yield a common temperature for a given fragmenting system. The inconsistent values of the real source temperature have also been commonly observed in the LCP temperature evaluation of the double isotope ratio thermometers after the quantitative sequential decay corrections [5,27,28]. This fact may be attributed to different reaction dynamics and fragment production mechanisms. The apparent temperature inherits this primary fluctuation, as indicated by the similar pattern of the T_{AMD} and $T_{app,AMD}$ values shown in Fig. 7. This is true for all other reactions in the AMD simulations discussed below. In contrast to the temperatures from the primary and secondary isotopes, the ΔT values for the eight thermometers show slightly smaller fluctuations from ∼−2 to ∼0 MeV, reflecting a cancellation for the effects of the reaction dynamics and the fragment production mechanisms. The remaining ΔT fluctuation may be attributed to the nuclear structure information for individual isotopes in the de-excitation process, as pointed out in Ref. [44].

In the present work, instead of using the double isotope thermometer as an absolute thermometer, we use it as a relative thermometer and divide the N/Z asymmetry dependence of the real source temperature into two effects. One is the N/Z asymmetry dependence of the apparent temperature, which has been discussed above, and the other is that of the relative temperature change between the apparent and real temperatures. To this end, we discuss the N/Z asymmetry dependence of ΔT using model simulations in the following subsection. Once we deduce the relation of ΔT vs source N/Z asymmetry, the N/Z asymmetry dependence of the real source temperature can be inferred from those of the apparent temperature and ΔT. A similar analysis procedure has already been applied to study the source N/Z asymmetry dependence of the nuclear caloric curve with the double isotope ratio thermometers by Sfienti *et al.* [5].

B. Qualitative sequential decay effect on N/Z asymmetry dependence of nuclear temperature

To model the fragmentation process, a number of theoretical models have been developed in two distinct scenarios. One scenario is based on transport theory in which nucleon propagation in a mean field and nucleon-nucleon collisions under Pauli-blocking are the two main physical processes. The other scenario assumes that the fragmentation takes place in equilibrated nuclear matter and the breakup configuration determined by statistical weights. We employ models for both scenarios, AMD used in the above sections and the statistical multifragmentation model (SMM) of Bondorf *et al.* [45]. For both calculations, the primary fragments are commonly identified as those directly from the fragmentation processes, and the secondary fragments are then generated using an afterburner. Different afterburners are employed in these two calculations. The GEMINI code of Charity *et al.* [37] is coupled with the AMD simulations, whereas the default encapsulated sequential decay code is used in SMM simulations. The system N/Z asymmetry in the AMD+GEMINI

calculations, $\delta_{\rm system}$, and source N/Z asymmetry in the SMM calculations, $\delta_{\rm source}$, are adopted to quantize the "source" N/Z asymmetry, δ, for a simplification. Note again that in the following analysis, the relative temperature change, ΔT, is defined as the difference between the temperatures from the secondary and primary isotope yields.

For the AMD+GEMINI analysis, the ^{58}Ti + ^{58}Ti, ^{58}Fe + ^{58}Fe, and ^{58}Ni + ^{58}Ni reaction systems at 40 MeV/nucleon are simulated. The lighter systems are chosen to mitigate the heavy CPU demand of the AMD simulations. The AMD simulations are performed with the Gogny interaction [46] and the Li-Machleidt in-medium nucleon-nucleon cross sections [47]. IMFs are identified at 300 fm/c using a coalescence technique with the radius of $R_c = 5$ in phase space and then transferred to GEMINI for de-excitations. Inclusive IMFs are used to calculate the yields from an impact parameter range of 0–8 fm. The resultant ΔT values as a function of δ are shown in Fig. 8. Errors are evaluated in the same way as in the data shown in Fig. 5. The global linear fit is also applied to the resultant AMD+GEMINI ΔT values. A weak dependence of ΔT on the source N/Z asymmetry is observed, although the absolute ΔT values fluctuate for the different thermometers. This can be attributed to the fact that the nuclear structure characteristics in the secondary decay process is the same for a given double isotope ratio selection among the reaction systems with different N/Z asymmetry, even if they are not fully taken into account. A common slope, $k_{\Delta T}^{\rm AMD} = -1.9 \pm 0.5$ MeV, is obtained from the fit. The negative sign of $k_{\Delta T}^{\rm AMD}$ is the same to that of the experimental value, $k_{\rm app}$ from Fig. 5. The absolute value of $k_{\Delta T}^{\rm AMD}$ is nearly four times larger than that of $k_{\rm app}$ but is still rather small, suggesting a weak N/Z asymmetry dependence of ΔT in the present AMD+GEMINI analysis. This $k_{\Delta T}^{\rm AMD}$ value has a consistent magnitude with the deduced $|k_{\Delta T}| \lesssim 2.5$ MeV from the previous observation reported by Sfienti *et al.* [5], in which the deviation of the secondary decay corrections is smaller than 300 keV as the projectile-like fragmenting source changes among ^{107}Sn, ^{124}La, and ^{124}Sn.

SMM is also utilized to simulate the fragmentation of $A = 100$ sources with different Z numbers, i.e., $Z = 35$, 40, 45, and 55. The fragmentation conditions are specified as excitation energies $E_x = 5$–10 MeV/nucleon and breakup densities $\rho/\rho_0 = 0.1$–0.2. The selection of $E_x = 5$–10 MeV/nucleon corresponds to the temperature range of 5-7 MeV examined in our previous work [48] and covers the temperature region which has been previously extracted from the IMF yields of the reaction ^{64}Zn + ^{112}Sn at 40 MeV/nucleon using a self-consistent method. In Fig. 9, the resultant ΔT vs δ relations under different initial fragmentation conditions are plotted for $E_x = 5$ MeV/nucleon and $\rho/\rho_0 = 0.1$ (circles), $E_x = 5$ MeV/nucleon and $\rho/\rho_0 = 0.2$ (squares), and $E_x = 10$ MeV/nucleon and $\rho/\rho_0 = 0.2$ (triangles). For the results under a given condition, the same global fit is applied, and three common slope values are obtained as $k_{\Delta T}^{\rm SMM} = -1.5 \pm 0.2$ MeV, -1.8 ± 0.2 MeV, and -1.3 ± 0.2 MeV, respectively. The consistency of these slope values strongly suggests a consistency of the N/Z asymmetry dependence of the sequential ΔT due to decay for source excitation energies and breakup densities. These slope values are also in rather good

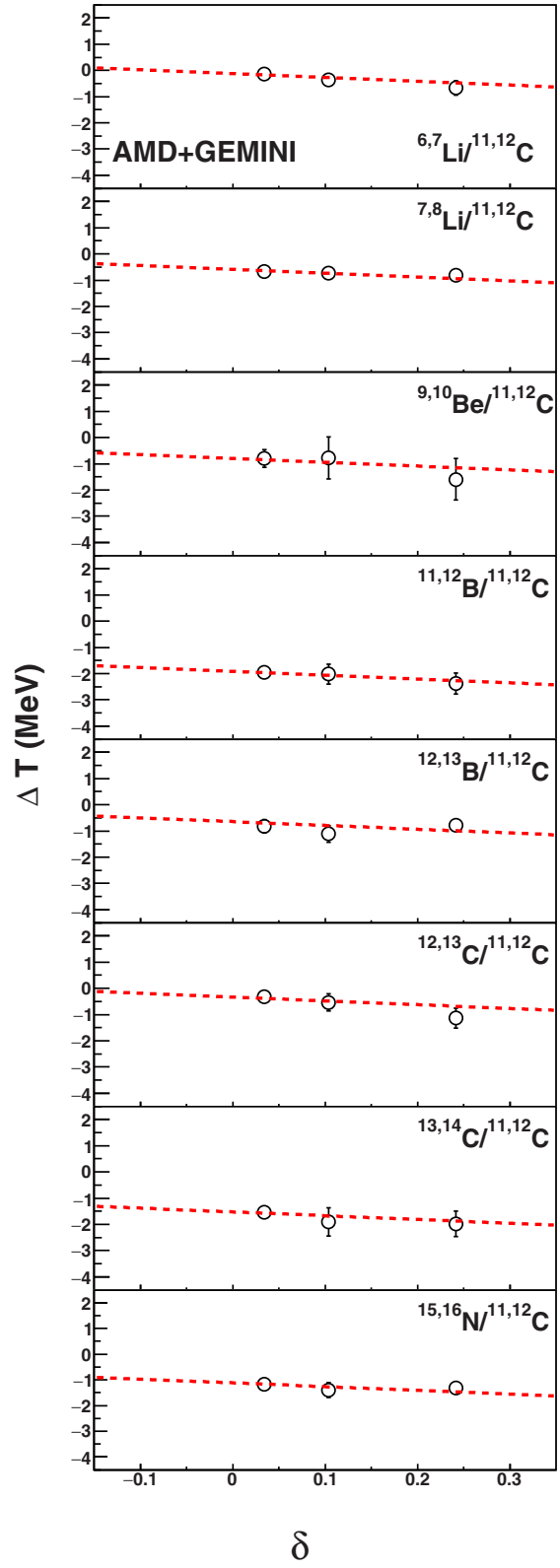

FIG. 8. Temperature difference ΔT between the temperatures from the secondary and primary isotope yields from the AMD+GEMINI simulations determined using the eight carbon-related thermometers as a function of δ. Red dashed lines represent the global fits with linear functions with one common slope $k_{\Delta T}^{\rm AMD}$ and different intercepts.

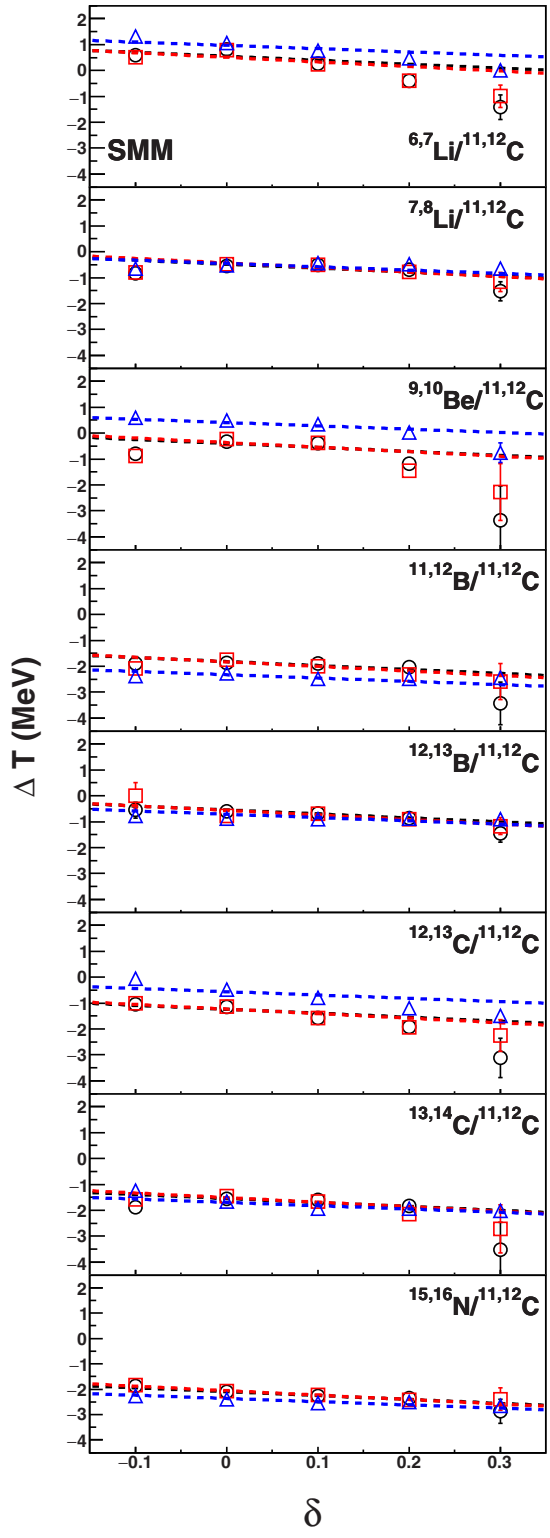

FIG. 9. Temperature difference ΔT between the temperatures from the secondary and primary isotope yields from the SMM simulations determined using the eight carbon-related thermometers as a function of δ. Initial fragmentation conditions are $E_x = 5$ MeV/nucleon and $\rho/\rho_0 = 0.1$ (circles), $E_x = 5$ MeV/nucleon and $\rho/\rho_0 = 0.2$ (squares), $E_x = 10$ MeV/nucleon and $\rho/\rho_0 = 0.2$ (triangles). Dashed lines represent the corresponding global fits with linear functions with one common slope $k_{\Delta T}^{\mathrm{SMM}}$ and different intercepts.

agreement with that of AMD+GEMINI, although AMD and SMM follow completely different fragmentation processes. It further confirms the weak dependence of the relative temperature change on the source N/Z asymmetry.

Combining the results in this section to the determined weak N/Z asymmetry dependence of the apparent temperature from the experimental IMF yields in the previous section, it can be inferred that the N/Z asymmetry dependence of the real source temperature from IMFs is very small. In the theoretical work of Refs. [49,50], Kolomietz *et al.* proposed that, a weak N/Z asymmetry dependence of temperature close to the phase transition appears under an equilibrium at a low pressure of $p = 10^{-2}$ MeV/fm^3 within the thermal Thomas-Fermi approximation. Similar conclusion was also reached by Hoel *et al.* [9]. Combining these theoretical predictions, the obtained weak N/Z asymmetry dependence of the real source temperature from IMFs favors a physical picture that IMFs are generated in a low-pressure configuration via a "soft" expansion.

C. Comparison with those from other work

In the following, we compare our results with those from other published work. We begin by describing and discussing the details of the experimental works.

(1) Kunde *et al.* [31] measured LCPs (d, t, ^{3}He, ^{4}He) from central collisions ($b/b_{\mathrm{max}} < 0.3$) of ^{124}Sn + ^{124}Sn and ^{112}Sn + ^{112}Sn at 40 MeV/nucleon with 280 plastic scintillator detectors of the Miniball/Miniwall array mounted in the Superball scattering chamber. The double isotope ratio thermometer with ^{2,3}H/^{3,4}He was employed. No correction for the sequential decay effect was made.

(2) Sfienti *et al.* [5] and Trautmann *et al.* [6] took measured particles from the projectile fragmentations of ^{124}Sn, ^{124}La, and ^{107}Sn on $^{\mathrm{nat}}$Sn at 600 MeV/nucleon as a probe. Charged particles were measured with the ALADIN forward spectrometer at SIS, GSI Darmstadt. Double isotope ratio thermometers with ^{6,7}Li/^{3,4}He and ^{9,7}Be/^{8,6}Li were utilized. The sequential decay effects were considered.

(3) McIntosh *et al.* [8] studied the N/Z asymmetry dependence of the nuclear caloric curve with the LCPs from the projectile fragmentation of ^{70}Zn + ^{70}Zn, ^{64}Zn + ^{64}Zn, and ^{58}Ni + ^{58}Ni at 35 MeV/nucleon. Both charged particles and associated neutrons were measured with the NIMROD-ISiS 4π detector array [51]. Excitation energies were determined from the reconstructed quasi-projectiles for noncentral collisions. The classical quadrupole momentum fluctuation thermometer [8] with protons was used to extract the temperature. No corrections for secondary decays was made with an assumption of a negligible contribution of the thermal energy in the primary clusters to the width of the quadrupole momentum [8].

Among above experiments, a negligible N/Z asymmetry dependence of the apparent temperature was observed by Kunde *et al.* and Sfienti *et al.*, in a good agreement with our present result. Sfienti *et al.*, as mentioned above, further pursued the dependence of secondary decay corrections on the source N/Z asymmetry, and found no significant N/Z asymmetry effects greater than 300 keV [5]. A negligible

N/Z asymmetry dependence of the real source temperature was therefore concluded. This conclusion has been used as experimental support for the assumption of N/Z asymmetry independence of the source temperature when the symmetry energy was extracted from isoscaling [52,53]. Different isotope ratios of LCPs and IMFs were used in the analysis procedures of Sfienti *et al.* and those of this work, but a consistent negligible N/Z asymmetry dependence of the source temperature is observed. This fact is an indication for early chemical equilibrium prior to the source fragmentation, since LCPs and IMFs involve different emission time scales in the collisions [54,55].

The temperatures evaluated by McIntosh *et al.* [8] show a notable decreasing trend as the source N/Z asymmetry increases, that is, the extracted quadrupole momentum fluctuation temperature values with protons are well described by a linear fit over the broad range of the source N/Z asymmetry with a slope of -7.3 MeV, independent of the source excitation energies [17]. The quadrupole momentum fluctuation temperature with heavier isotopes show even larger slopes [17], -14.6 MeV slope for ^{9}Be for instance. However, it should also be mentioned that an earlier measurement of the same group with $^{86,78}\mathrm{Kr} + {}^{64,58}\mathrm{Ni}$ at 35 MeV/nucleon was performed by Wuenschel *et al.* [7], and the obtained temperatures do not show a significant N/Z asymmetry dependence as those obtained by McIntosh *et al.* in Refs. [8,17], where the same quadrupole momentum fluctuation thermometers were applied. In Ref. [17], they pointed out that the absence of the N/Z asymmetry dependence of the temperature is due to the inaccurate quasiprojectile source selection in the experiment of Wuenschel *et al.* [8], and that if the quasiprojectile sources are selected properly, a similar result is expected. Later, McIntosh *et al.* also applied the double isotope ratio thermometers ($^{2,3}\mathrm{H}/^{3,4}\mathrm{He}$ and $^{6,7}\mathrm{Li}/^{3,4}\mathrm{He}$) to the same data set [17]. In contrast to those from quadrupole momentum fluctuation thermometers, the extracted apparent temperatures become much less dependent on the source N/Z asymmetry with a slope value around -0.9 MeV, in good agreement with our present results in order of magnitudes. The significant magnitude difference of the results from double isotope ratio thermometer and quadrupole momentum fluctuation thermometer from above comparison indicates a sensitivity of temperature N/Z asymmetry dependence to the thermometer used [17], and further reveals a requirement for a systematic benchmark study for nuclear thermometers prior to studying the dependence properties of nuclear temperature in future.

VI. SUMMARY

The N/Z asymmetry dependence of the nuclear temperature is experimentally investigated with the IMF isotopes produced from thirteen reaction systems with different N/Z asymmetries, ^{64}Zn on ^{112}Sn and ^{70}Zn, ^{64}Ni on ^{112,124}Sn, ^{58,64}Ni, ^{197}Au, ^{232}Th at 40 MeV/nucleon. The apparent temperatures for these systems are determined from the measured IMF yields from the IV sources using eight carbon-related double isotope ratio thermometers. A rather negligible N/Z asymmetry dependence of the extracted apparent temperature is observed in the N/Z asymmetry range from 0.14 to 0.27. To take into account the alteration of the measured isotope yields by sequential decay, the N/Z asymmetry dependence of the relative temperature change, which is defined as the difference between the temperatures from secondary and primary isotope yields, is investigated using the AMD+GEMINI and SMM simulations. The real source temperature is then qualitatively inferred to have a rather weak dependence on the source N/Z asymmetry. The present result is compared with those from other independent experiments. It is found that the temperature deduced from the double isotope ratio thermometers commonly shows a small N/Z asymmetry dependence, consistent with results using thermometers with LCPs and IMFs. In contrast, the temperature in another experiment deduced from the quadrupole momentum fluctuation thermometers shows a significant decrease with increasing the source N/Z asymmetry.

ACKNOWLEDGMENTS

The authors thank the operational staff in the cyclotron Institute, Texas A&M University, for their support during the experiment. The authors thank A. Ono and A. S. Botvina for providing their codes (AMD and SMM). This work is supported by the National Natural Science Foundation of China (Grants No. 11705242, No. U1632138, No. 11805138, No. 11905120, No. 11775273, No. 11575269, and No. 11775013), the Fundamental Research Funds For the Central Universities (Grants No. YJ201954, No. YJ201820, and No. GK201903022) in China, the CAS Pioneer Hundred Talents Program and the National MCF Energy R&D Program of China (Grant No. 2018YFE0310200). This work is also supported by the US Department of Energy under Grant No. DE-FG02-93ER40773.

[1] W. A. Friedman, Phys. Rev. Lett. **60**, 2125 (1988).
[2] E. Suraud, C. Gregoire, and B. Tamain, Prog. Part. Nucl. Phys. **23**, 357 (1989).
[3] D. Gross *et al.*, Prog. Part. Nucl. Phys. **30**, 155 (1993).
[4] B.-A. Li, L.-W. Chen, and C. M. Ko, Phys. Rep. **464**, 113 (2008).
[5] C. Sfienti *et al.*, Phys. Rev. Lett. **102**, 152701 (2009).
[6] W. Trautmann *et al.*, Int. J. Mod. Phys. E **17**, 1838 (2008).
[7] S. Wuenschel *et al.*, Nucl. Phys. A **843**, 1 (2010).
[8] A. B. McIntosh *et al.*, Phys. Lett. B **719**, 337 (2013).
[9] C. Hoel, L. G. Sobotka, and R. J. Charity, Phys. Rev. C **75**, 017601 (2007).
[10] J. Besprosvany and S. Levit, Phys. Lett. B **217**, 1 (1989).
[11] R. Ogul and A. S. Botvina, Phys. Rev. C **66**, 051601(R) (2002).
[12] J. Su and F. S. Zhang, Phys. Rev. C **84**, 037601 (2011).
[13] F. Zhang, C. Li, L. Zhu, H. Liu, and F. S. Zhang, Phys. Rev. C **91**, 034617 (2015).
[14] T. X. Liu *et al.*, Europhys. Lett. **74**, 806 (2006).
[15] W. A. Friedman and W. G. Lynch, Phys. Rev. C **28**, 16 (1983).
[16] S. R. Souza and R. Donangelo, Phys. Rev. C **97**, 054619 (2018).

[17] A. B. McIntosh *et al.*, Eur. Phys. J. A **50**, 35 (2014).
[18] J. B. Natowitz, R. Wada, K. Hagel, T. Keutgen, M. Murray, A. Makeev, L. Qin, P. Smith, and C. Hamilton, Phys. Rev. C **65**, 034618 (2002).
[19] B. Borderie and M. F. Rivet, Prog. Part. Nucl. Phys. **61**, 551 (2008).
[20] W. Lin, X. Liu, M. R. D. Rodrigues, S. Kowalski, R. Wada, M. Huang, S. Zhang, Z. Chen, J. Wang, G. Q. Xiao, R. Han, Z. Jin, J. Liu, F. Shi, T. Keutgen, K. Hagel, M. Barbui, C. Bottosso, A. Bonasera, J. B. Natowitz, E. J. Kim, T. Materna, L. Qin, P. K. Sahu, K. J. Schmidt, S. Wuenschel, and H. Zheng, Phys. Rev. C **89**, 021601(R) (2014).
[21] W. Lin *et al.*, Phys. Rev. C **90**, 044603 (2014).
[22] X. Liu *et al.*, Phys. Rev. C **90**, 014605 (2014).
[23] X. Liu *et al.*, Nucl. Phys. A **933**, 290 (2015).
[24] X. Liu, H. Zheng, W. Lin, M. Huang, Y. Y. Yang, J. S. Wang, R. Wada, A. Bonasera, and J. B. Natowitz, Phys. Rev. C **97**, 014613 (2018).
[25] X. Liu *et al.*, Phys. Rev. C **92**, 014623 (2015).
[26] S. Albergo, *et al.* Nuovo Cimento A **89**, 1 (1985).
[27] W. Trautmann *et al.*, Phys. Rev. C **76**, 064606 (2007).
[28] H. Xi, W. G. Lynch, M. B. Tsang, W. A. Friedman, and D. Durand, Phys. Rev. C **59**, 1567 (1999).
[29] H. F. Xi, G. J. Kunde, O. Bjarki, C. K. Gelbke, R. C. Lemmon, W. G. Lynch, D. Magestro, R. Popescu, R. Shomin, M. B. Tsang, A. M. Vandermolen, G. D. Westfall, G. Imme, V. Maddalena, C. Nociforo, G. Raciti, G. Riccobene, F. P. Romano, A. Saija, C. Sfienti, S. Fritz, C. Gross, T. Odeh, C. Schwarz, A. Nadasen, D. Sisan, and K. A. G. Rao, Phys. Rev. C **58**, R2636 (1998).
[30] V. Serfling *et al.*, Phys. Rev. Lett. **80**, 3928 (1998).
[31] G. J. Kunde *et al.*, Phys. Lett B **416**, 56 (1998).
[32] J. Wang *et al.*, Phys. Rev. C **72**, 024603 (2005).
[33] F. Hubert, R. Bimbot, and H. Gauvin, At. Data Nucl. Data Tables **46**, 1 (1990).
[34] I. Tilquin *et al.*, Nucl. Instrum. Methods Phys. Res., Sect. A **365**, 446 (1995).
[35] M. R. D. Rodrigues, W. Lin, X. Liu, M. Huang, S. Zhang, Z. Chen, J. Wang, R. Wada, S. Kowalski, T. Keutgen, K. Hagel, M. Barbui, C. Bottosso, A. Bonasera, J. B. Natowitz, T. Materna, L. Qin, P. K. Sahu, and K. J. Schmidt, Phys. Rev. C **88**, 034605 (2013).
[36] A. Ono, Phys. Rev. C **59**, 853 (1999).
[37] R. J. Charity *et al.*, Nucl. Phys. A **483**, 371 (1988).
[38] R. Wada *et al.*, Phys. Rev. C **69**, 044610 (2004).
[39] M. Huang *et al.*, Phys. Rev. C **82**, 054602 (2010).
[40] T. C. Awes, G. Poggi, C. K. Gelbke, B. B. Back, B. G. Glagola, H. Breuer, and V. E. Viola, Phys. Rev. C **24**, 89 (1981).
[41] Z. Chen *et al.*, Phys. Rev. C **81**, 064613 (2010).
[42] See Supplemental Material at http://link.aps.org/supplemental/10.1103/PhysRevC.100.064601 for the experimentally extracted neutron and LCP and IMF yields from IV sources for all thirteen systems.
[43] M. B. Tsang, W. G. Lynch, H. Xi, and W. A. Friedman, Phys. Rev. Lett. **78**, 3836 (1997).
[44] S. Das Gupta, A. Z. Mekjian, and M. B. Tsang, Adv. Nucl. Phys. **26**, 89 (2001).
[45] J. Bondorf, A. S. Botvina, A. S. Iljinov, I. N. Mishutin, and K. Sneppen, Phys. Rep. **257**, 133 (1995).
[46] A. Ono and H. Horiuchi, Prog. Part. Nucl. Phys. **53**, 501 (2004).
[47] G. Q. Li and R. Machleidt, Phys. Rev. C **49**, 566 (1994).
[48] W. Lin, P. Ren, H. Zheng, X. Liu, M. Huang, K. Yang, G. Qu, and R. Wada, Phys. Rev. C **99**, 054616 (2019).
[49] V. M. Kolomietz, A. I. Sanzhur, S. Shlomo, and S. A. Firin, Phys. Rev. C **64**, 024315 (2001).
[50] S. Shlomo and V. M. Kolomietz, Rep. Prog. Phys. **68**, 1 (2005).
[51] S. Wuenschel *et al.*, Nucl. Instrum. Methods Phys. Res., Sect. A **604**, 578 (2009).
[52] H. S. Xu *et al.*, Phys. Rev. Lett. **85**, 716 (2000).
[53] M. B. Tsang *et al.*, Phys. Rev. C **64**, 054615 (2001).
[54] F. Z. Ighezou *et al.*, Nucl. Phys. A **662**, 295 (2000).
[55] L. Beaulieu *et al.*, Phys. Rev. Lett. **84**, 5971 (2000).